

Chapter 2

ELECTRON OPTICS

Chapter 1 contained an overview of various forms of microscopy, carried out using light, electrons, and mechanical probes. In each case, the microscope forms an enlarged image of the original object (the specimen) in order to convey its internal or external structure. Before dealing in more detail with various forms of electron microscopy, we will first examine some general concepts behind image formation. These concepts were derived during the development of visible-light optics but have a range of application that is much wider.

2.1 Properties of an Ideal Image

Clearly, an optical image is closely related to the corresponding object, but what does this mean? What properties should the image have in relation to the object? The answer to this question was provided by the Scottish physicist James Clark Maxwell, who also developed the equations relating electric and magnetic fields that underlie all electrostatic and magnetic phenomena, including electromagnetic waves. In a journal article (Maxwell, 1858), remarkable for its clarity and for its frank comments about fellow scientists, he stated the requirements of a perfect image as follows

1. For each point in the object, there is an **equivalent** point in the image.
2. The object and image are geometrically **similar**.
3. If the object is **planar** and perpendicular to the optic axis, so is the image.

Besides defining the desirable properties of an image, Maxwell's principles are useful for categorizing the **image defects** that occur (in practice) when the image is *not* ideal. To see this, we will discuss each rule in turn.

Rule 1 states that for each point in the object we can define an *equivalent* point in the image. In many forms of microscopy, the connection between these two points is made by some kind of particle (*e.g.*, electron or photon) that leaves the object and ends up at the related image point. It is conveyed from object to image through a focusing device (such as a lens) and its trajectory is referred to as a **ray** path. One particular ray path is called the **optic axis**; if no mirrors are involved, the optic axis is a straight line passing through the center of the lens or lenses.

How closely this rule is obeyed depends on several properties of the lens. For example, if the focusing *strength* is incorrect, the image formed at a particular plane will be **out-of-focus**. Particles leaving a single point in the object then arrive anywhere within a circle *surrounding* the ideal-image point, a so-called **disk of confusion**. But even if the focusing power is appropriate, a real lens can produce a disk of confusion because of lens **aberrations**: particles having different energy, or which take different paths after leaving the object, arrive displaced from the “ideal” image point. The image then appears blurred, with loss of fine detail, just as in the case of an out-of-focus image.

Rule 2: If we consider object points that form a pattern, their equivalent points in the image should form a similar pattern, rather than being distributed at random. For example, any three object points define a triangle and their locations in the image represent a triangle that is *similar* in the geometric sense: it contains the same angles. The image triangle may have a different orientation than that of the object triangle; for example it could be **inverted** (relative to the optic axis) without violating Rule 2, as in Fig. 2-1. Also, the separations of the three image points may differ from those in the object by a **magnification factor** M , in which case the image is **magnified** (if $M > 1$) or **demagnified** (if $M < 1$).

Although the light image formed by a glass lens may appear similar to the object, close inspection often reveals the presence of **distortion**. This effect is most easily observed if the object contains straight lines, which appear as curved lines in the distorted image.

The presence of image distortion is equivalent to a variation of the magnification factor with *position* in the object or image: **pincushion** distortion corresponds to M increasing with radial distance away from the optic axis (Fig. 2-2a), **barrel** distortion corresponds to M decreasing away from the axis (Fig. 2-2b). As we will see, many electron lenses cause a *rotation* of the image, and if this rotation increases with distance from the axis, the result is **spiral** distortion (Fig. 2-2c).

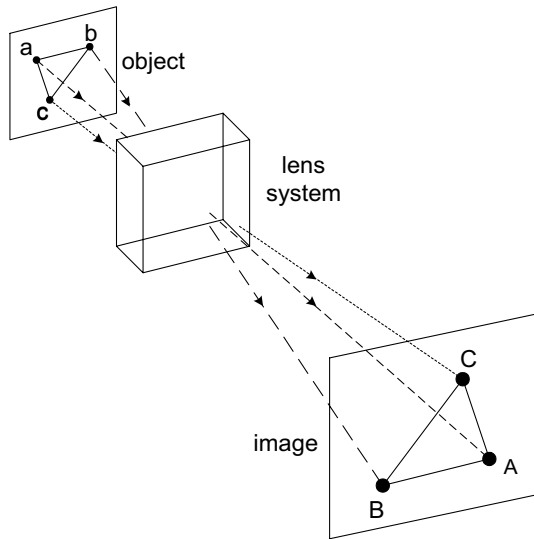


Figure 2-1. A triangle imaged by an ideal lens, with magnification and inversion. Image points A, B, and C are equivalent to the object points a, b, and c, respectively.

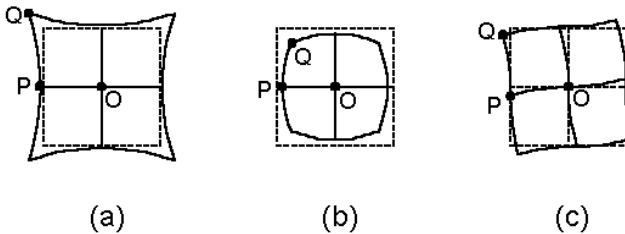


Figure 2-2. (a) Square mesh (dashed lines) imaged with pincushion distortion (solid curves); magnification M is higher at point Q than at point P. (b) Image showing barrel distortion, with M at Q lower than at P. (c) Image of a square, showing spiral distortion; the counterclockwise rotation is higher at Q than at P.

Rule 3: Images usually exist in two dimensions and occupy a *flat* plane. Even if the corresponding object is three-dimensional, only a single object plane is *precisely* in focus in the image. In fact, lenses are usually evaluated using a flat test chart and the sharpest image should ideally be produced on a flat screen. But if the focusing power of a lens depends on the distance of an object point from the optic axis, different regions of the image are brought to focus at different distances from the lens. The optical system then suffers from **curvature of field**; the sharpest image would be formed on a surface

that is curved rather than planar. Inexpensive cameras have sometimes compensated for this lens defect by curving the photographic film. Likewise, the Schmidt astronomical telescope installed at Mount Palomar was designed to record a well-focused image of a large section of the sky on 14-inch square glass plates, bent into a section of a sphere using vacuum pressure.

To summarize, focusing aberrations occur when Maxwell's Rule 1 is broken: the image appears blurred because rays coming from a single point in the object are focused into a *disk* rather than a single point in the image plane. Distortion occurs when Rule 2 is broken, due to a change in image magnification (or rotation) with position in the object plane. Curvature of field occurs when Rule 3 is broken, due to a change in focusing power with position in the object plane.

2.2 Imaging in Light Optics

Because electron optics makes use of many of the concepts of light optics, we will quickly review some of the basic optical principles. In light optics, we can employ a glass lens for focusing, based on the property of **refraction**: deviation in direction of a light ray at a boundary where the **refractive index** changes. Refractive index is inversely related to the *speed* of light, which is $c = 3.00 \times 10^8$ m/s in vacuum (and almost the same in air) but c/n in a transparent material (such as glass) of refractive index n . If the angle of incidence (between the ray and the perpendicular to an air/glass interface) is θ_1 in air ($n_1 \approx 1$), the corresponding value θ_2 in glass ($n_2 \approx 1.5$) is smaller by an amount given by Snell's law:

$$n_1 \sin \theta_1 = n_2 \sin \theta_2 \quad (2.1)$$

Refraction can be demonstrated by means of a glass prism; see Fig. 2-3. The total deflection angle α , due to refraction at the air/glass *and* the glass/air interfaces, is independent of the thickness of the glass, but increases with increasing prism angle ϕ . For $\phi = 0$, corresponding to a flat sheet of glass, there is no overall angular deflection ($\alpha = 0$).

A **convex lens** can be regarded as a prism whose angle increases with distance away from the optic axis. Therefore, rays that arrive at the lens far from the optic axis are deflected more than those that arrive close to the axis (the so-called **paraxial** rays). To a first approximation, the deflection of a ray is proportional to its distance from the optic axis (at the lens), as needed to make rays starting from an on-axis object point *converge* toward a single (on-axis) point in the image (Fig. 2-4) and therefore satisfy the first of Maxwell's rules for image formation.

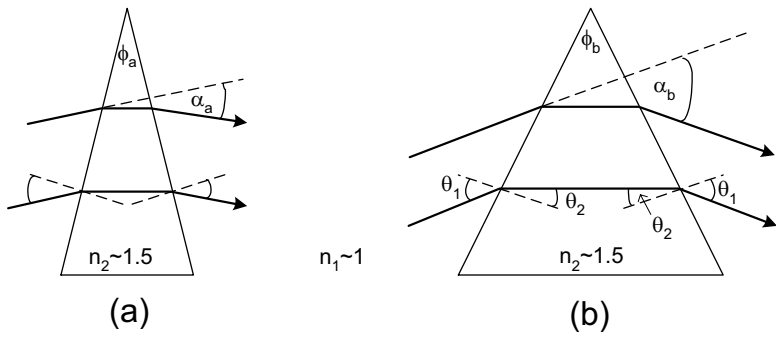


Figure 2-3. Light refracted by a glass prism (a) of small angle ϕ_a and (b) of large angle ϕ_b . Note that the angle of deflection α is independent of the glass thickness but increases with increasing prism angle.

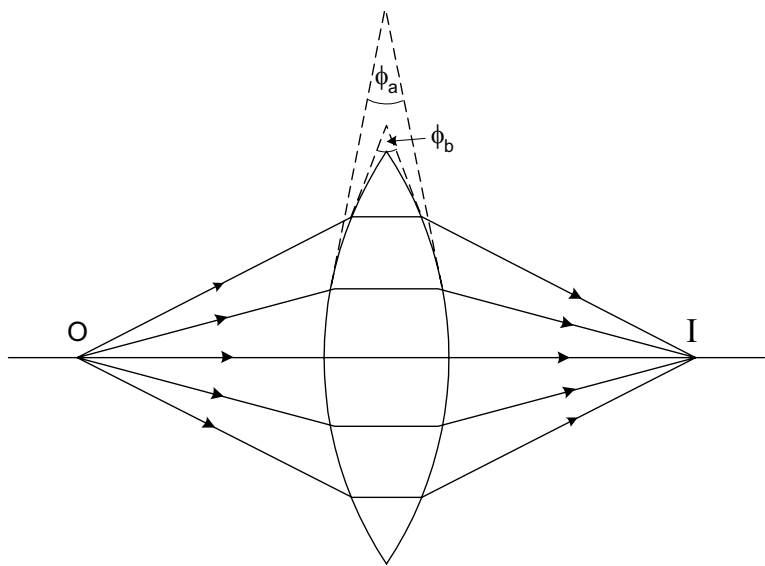


Figure 2-4. A convex lens focusing rays from axial object point O to an axial image point I .

In Fig. 2-4, we have shown only rays that originate from a *single point* in the object, which happens to lie on the optic axis. In practice, rays originate from all points in the two-dimensional object and may travel at various angles relative to the optic axis. A ray diagram that showed *all* of these rays

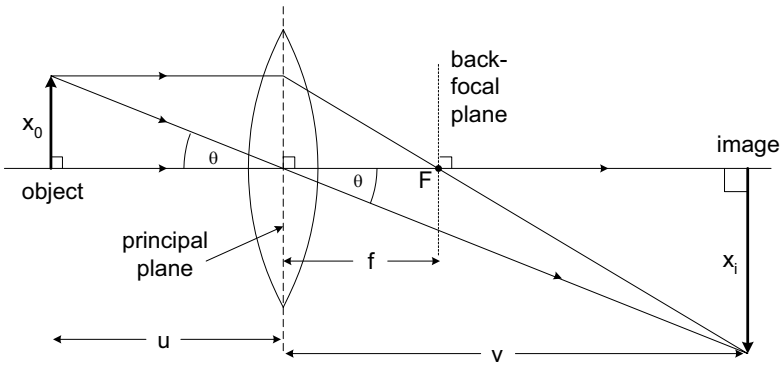


Figure 2-5. A thin-lens ray diagram, in which bending of light rays is imagined to occur at the mid-plane of the lens (dashed vertical line). These special rays define the focal length f of the lens and the location of the back-focal plane (dotted vertical line).

would be highly confusing, so in practice it is sufficient to show just a few *special* rays, as in Fig. 2-5.

One special ray is the one that travels *along* the optic axis. Because it passes through the center of the lens, where the prism angle is zero, this ray does not deviate from a straight line. Similarly, an oblique ray that leaves the object at a distance X_0 from the optic axis but happens to pass through the *center of the lens*, remains unchanged in direction. A third example of a special ray is one that leaves the object at distance X_0 from the axis and travels *parallel to* the optic axis. The lens bends this ray toward the optic axis, so that it crosses the axis at point F, a distance f (the **focal length**) from the center of the lens. The plane, perpendicular to the optic axis and passing through F, is known as the **back-focal plane** of the lens.

In drawing ray diagrams, we are using **geometric optics** to depict the image formation. Light is represented by rays rather than waves, and so we ignore any diffraction effects (which would require **physical optics**).

It is convenient if we can assume that the bending of light rays takes place at a single plane (known as the **principal plane**) perpendicular to the optic axis (dashed line in Fig. 2-5). This assumption is reasonable if the radii of curvature of the lens surfaces are large compared to the focal length, which implies that the lens is *physically* thin, and is therefore known as the **thin-lens approximation**. Within this approximation, the object distance u and the image distance v (both measured from the principal plane) are related to the focal length f by the thin-lens equation:

$$1/u + 1/v = 1/f \quad (2.2)$$

We can define image magnification as the ratio of the lengths X_i and X_o , measured perpendicular to the optic axis. Because the two triangles defined in Fig. 2-5 are similar (both contain a right angle and the angle θ), the ratios of their horizontal and vertical dimensions must be equal. In other words,

$$v/u = X_i/X_o = M \quad (2.3)$$

From Fig. 2-5, we see that if a single lens forms a **real image** (one that could be viewed by inserting a screen at the appropriate plane), this image is *inverted*, equivalent to a 180° rotation about the optic axis. If a second lens is placed beyond this real image, the latter acts as an *object* for the *second* lens, which produces a *second* real image that is upright (not inverted) relative to the original object. The location of this second image is given by applying Eq. (2.2) with appropriate new values of u and v , while the additional magnification produced by the second lens is given by applying Eq. (2.3). The *total* magnification (between second image and original object) is then the *product* of the magnification factors of the two lenses.

If the second lens is placed *within* the image distance of the first, a real image cannot be formed but, the first lens is said to form a **virtual image**, which acts as a virtual *object* for the second lens (having a *negative* object distance u). In this situation, the first lens produces *no* image inversion. A familiar example is a magnifying glass, held within its focal length of the object; there is no inversion and the only real image is that produced on the retina of the eye, which the brain *interprets* as upright.

Most glass lenses have *spherical* surfaces (sections of a sphere) because these are the easiest to make by grinding and polishing. Such lenses suffer from **spherical aberration**, meaning that rays arriving at the lens at larger distances from the optic axis are focused to points that differ from the focal point of the paraxial rays. Each image point then becomes a disk of confusion, and the image produced on any given plane is blurred (reduced in resolution, as discussed in Chapter 1). *Aspherical* lenses have their surfaces tailored to the precise shape required for ideal focusing (for a given object distance) but are more expensive to produce.

Chromatic aberration arises when the light being focused has more than one wavelength present. A common example is white light that contains a continuous range of wavelengths between its red and violet components. Because the refractive index of glass varies with wavelength (called **dispersion**, as it allows a glass prism to *separate* the component colors of the white light), the focal length f and the image distance v are slightly different for each wavelength present. Again, each object point is broadened into a disk of confusion and image sharpness is reduced.

2.3. Imaging with Electrons

Electron optics has much in common with light optics. We can imagine individual electrons leaving an object and being focused into an image, analogous to visible-light photons. As a result of this analogy, each electron trajectory is often referred to as a *ray* path.

To obtain the equivalent of a convex lens for electrons, we must arrange for the amount of deflection to increase with increasing deviation of the electron ray from the optic axis. For such focusing, we cannot rely on refraction by a material such as glass, as electrons are strongly scattered and absorbed soon after entering a solid. Instead, we take advantage of the fact that the electron has an electrostatic charge and is therefore deflected by an electric field. Alternatively, we can use the fact that the electrons in a beam are moving; the beam is therefore equivalent to an electric current in a wire, and can be deflected by an applied magnetic field.

Electrostatic lenses

The most straightforward example of an electric field is the uniform field produced between two parallel conducting plates. An electron entering such a field would experience a constant force, regardless of its trajectory (ray path). This arrangement is suitable for *deflecting* an electron beam, as in a cathode-ray tube, but not for focusing.

The simplest electrostatic *lens* consists of a circular conducting electrode (disk or tube) connected to a negative potential and containing a circular hole (aperture) centered about the optic axis. An electron passing *along* the optic axis is repelled equally from all points on the electrode and therefore suffers no deflection, whereas an off-axis electron is repelled by the negative charge that lies closest to it and is therefore deflected back toward the axis, as in Fig. 2-6. To a first approximation, the deflection angle is proportional to displacement from the optic axis and a point source of electrons is focused to a single image point.

A practical form of electrostatic lens (known as a **unipotential** or *einzel* lens, because electrons enter and leave it at the same potential) uses additional electrodes placed before and after, to limit the extent of the electric field produced by the central electrode, as illustrated in Fig. 2-5. Note that the electrodes, and therefore the electric fields which give rise to the focusing, have cylindrical or **axial symmetry**, which ensures that the focusing force depends only on *radial* distance of an electron from the axis and is independent of its *azimuthal* direction *around* the axis.

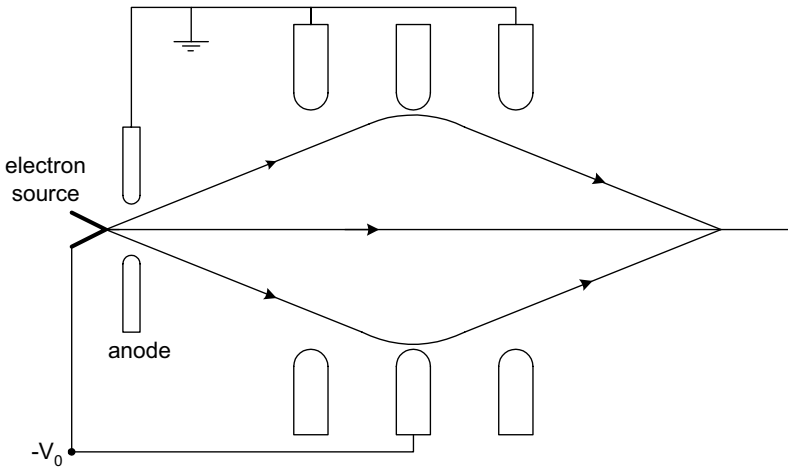


Figure 2-6. Electrons emitted from an electron source, accelerated through a potential difference V_0 toward an anode and then focused by a unipotential electrostatic lens. The electrodes, seen here in cross section, are circular disks containing round holes (apertures) with a common axis, the optic axis of the lens.

Electrostatic lenses have been used in cathode-ray tubes and television picture tubes, to ensure that the electrons emitted from a heated filament are focused back into a small spot on the phosphor-coated inside face of the tube. Although some early electron microscopes used electrostatic lenses, modern electron-beam instruments use electromagnetic lenses that do not require high-voltage insulation and have somewhat lower aberrations.

Magnetic lenses

To focus an electron beam, an electromagnetic lens employs the magnetic field produced by a coil carrying a direct current. As in the electrostatic case, a *uniform* field (applied perpendicular to the beam) would produce overall deflection but no focusing action. To obtain focusing, we need a field with axial symmetry, similar to that of the einzel lens. Such a field is generated by a short coil, as illustrated in Fig. 2-7a. As the electron passes through this non-uniform magnetic field, the force acting on it varies in both magnitude and direction, so it must be represented by a vector quantity \mathbf{F} . According to electromagnetic theory,

$$\mathbf{F} = -e (\mathbf{v} \times \mathbf{B}) \quad (2.4)$$

In Eq. (2.4), $-e$ is the negative charge of the electron, \mathbf{v} is its velocity vector and \mathbf{B} is the magnetic field, representing both the magnitude B of the field (or induction, measured in Tesla) and its direction. The symbol \times indicates a

cross-product or **vector product** of \mathbf{v} and \mathbf{B} ; this mathematical operator gives Eq. (2.4) the following two properties.

1. The direction of \mathbf{F} is *perpendicular* to both \mathbf{v} and \mathbf{B} . Consequently, \mathbf{F} has *no* component in the direction of motion, implying that the electron speed v (the *magnitude* of the velocity \mathbf{v}) remains constant at all times. But because the direction of \mathbf{B} (and possibly \mathbf{v}) changes continuously, so does the direction of the magnetic force.
2. The magnitude F of the force is given by:

$$F = e v B \sin(\varepsilon) \quad (2.5)$$

where ε is the instantaneous angle between \mathbf{v} and \mathbf{B} at the location of the electron. Because B (and possibly v) changes continuously as an electron passes through the field, so does F . Note that for an electron traveling along the coil axis, \mathbf{v} and \mathbf{B} are always in the axial direction, giving $\varepsilon = 0$ and $F = 0$ at every point, implying no deviation of the ray path from a straight line. Therefore, the symmetry axis of the magnetic field is the optic axis.

For non-axial trajectories, the motion of the electron is more complicated. It can be analyzed in detail by using Eq. (2.4) in combination with Newton's second law ($\mathbf{F} = m \, d\mathbf{v}/dt$). Such analysis is simplified by considering \mathbf{v} and \mathbf{B} in terms of their vector components. Although we could take components parallel to three perpendicular axes (x , y , and z), it makes more sense to recognize from the outset that the magnetic field possesses axial (cylindrical)

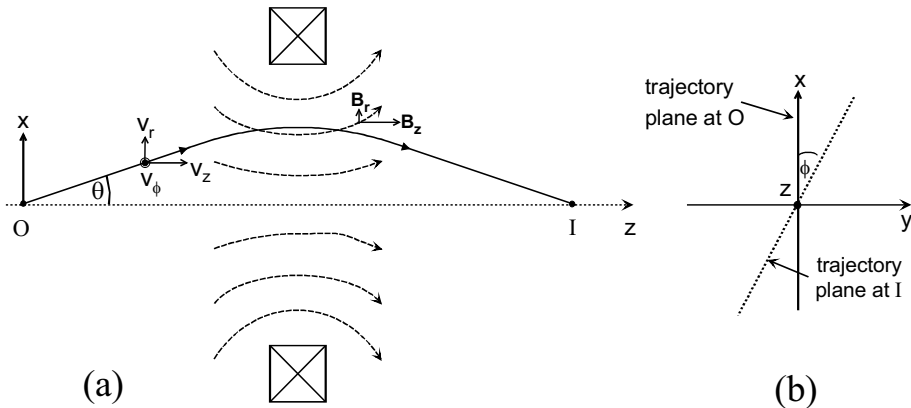


Figure 2-7. (a) Magnetic flux lines (dashed curves) produced by a short coil, seen here in cross section, together with the trajectory of an electron from an axial object point O to the equivalent image point I. (b) View along the z -direction, showing rotation ϕ of the plane of the electron trajectory, which is also the rotation angle for an extended image produced at I.

symmetry and use cylindrical coordinates: z , r (= radial distance away from the z -axis) and ϕ (= azimuthal angle, representing the direction of the radial vector \mathbf{r} relative to the plane of the initial trajectory). Therefore, as shown in Fig. (2-7a), v_z , v_r and v_ϕ are the axial, radial, and tangential components of electron velocity, while B_z and B_r are the axial and radial components of magnetic field. Equation (2.5) can then be rewritten to give the tangential, radial, and axial components of the magnetic force on an electron:

$$F_\phi = -e (v_z B_r) + e (B_z v_r) \quad (2.6a)$$

$$F_r = -e (v_\phi B_z) \quad (2.6b)$$

$$F_z = e (v_\phi B_r) \quad (2.6c)$$

Let us trace the path of an electron that starts from an axial point O and enters the field at an angle θ , defined in Fig. 2-7, relative to the symmetry (z) axis. As the electron approaches the field, the main component is B_r and the predominant force comes from the term $(v_z B_r)$ in Eq. (2.6a). Since B_r is negative (field lines *approach* the z -axis), this contribution $(-e v_z B_r)$ to F_ϕ is positive, meaning that the tangential force F_ϕ is clockwise, as viewed along the $+z$ direction. As the electron approaches the center of the field ($z = 0$), the magnitude of B_r decreases but the second term $e(B_z v_r)$ in Eq. (2.6a), also positive, increases. So as a result of both terms in Eq. (2.6a), the electron starts to spiral through the field, acquiring an increasing tangential velocity v_ϕ directed *out* of the plane of Fig. (2-7a). Resulting from this acquired tangential component, a new force F_r starts to act on the electron. According to Eq. (2.6b), this force is negative (toward the z -axis), therefore we have a focusing action: the non-uniform magnetic field acts like a convex lens.

Provided that the radial force F_r toward the axis is large enough, the radial motion of the electron will be *reversed* and the electron will approach the z -axis. Then v_r becomes negative and the *second* term in Eq. (2.6a) becomes negative. And after the electron passes the $z = 0$ plane (the center of the lens), the field lines start to diverge so that B_r becomes positive and the *first* term in Eq. (2.6a) also becomes negative. As a result, F_ϕ becomes negative (reversed in direction) and the tangential velocity v_ϕ falls, as shown in Fig. 2-8c; by the time the electron leaves the field, its spiraling motion is reduced to zero. However, the electron is now traveling in a plane that has been *rotated* relative to its original (x - z) plane; see Fig. 2-7b.

This rotation effect is *not* depicted in Fig (2.7a) or in the other ray diagrams in this book, where for convenience we plot the radial distance r of the electron (from the axis) as a function of its axial distance z . This common convention allows the use of two-dimensional rather than three-dimensional diagrams; by effectively suppressing (or ignoring) the rotation effect, we can draw ray diagrams that resemble those of light optics. Even so, it is

important to remember that the trajectory has a rotational component whenever an electron passes through an axially-symmetric magnetic lens.

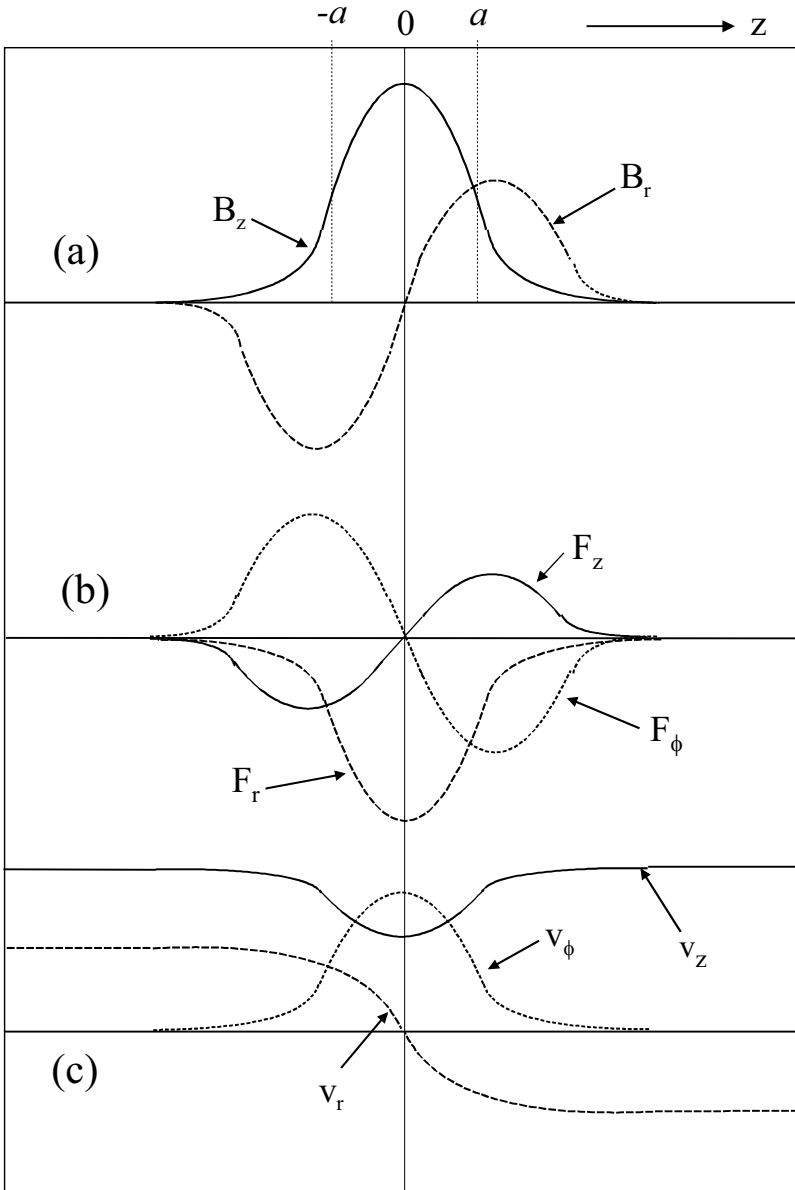


Figure 2-8. Qualitative behavior of the radial (r), axial (z), and azimuthal (ϕ) components of (a) magnetic field, (b) force on an electron, and (c) the resulting electron velocity, as a function of the z -coordinate of an electron going through the electron lens shown in Fig. 2-7a.

As we said earlier, the overall speed v of an electron in a magnetic field remains constant, so the appearance of tangential and radial components of velocity implies that v_z must decrease, as depicted in Fig. 2-8c. This is in accordance with Eq. (2.6c), which predicts the existence of a third force F_z which is negative for $z < 0$ (because $B_r < 0$) and therefore acts in the $-z$ direction. After the electron passes the center of the lens, z , B_r and F_z all become positive and v_z increases back to its original value. The fact that the electron speed is constant contrasts with the case of the einzel electrostatic lens, where an electron slows down as it passes through the retarding field.

We have seen that the radial component of magnetic induction B_r plays an important part in electron focusing. If a long coil (solenoid) were used to generate the field, this component would be present only in the **fringing field** at either end. (The uniform field inside the solenoid can focus electrons radiating from a point source but not a broad beam of electrons traveling parallel to its axis). So rather than using an *extended* magnetic field, we should make the field as short as possible. This can be done by partially enclosing the current-carrying coil by ferromagnetic material such as soft iron, as shown in Fig. 2-9a. Due to its high permeability, the iron carries most of the magnetic flux lines. However, the magnetic circuit contains a **gap** filled with nonmagnetic material, so that flux lines appear within the internal **bore** of the lens. The magnetic field experienced by the electron beam can be increased and further concentrated by the use of ferromagnetic (soft iron) **polepieces** of small internal diameter, as illustrated in Fig. 2-9b. These polepieces are machined to high precision to ensure that the magnetic field has the high degree of axial symmetry required for good focusing.

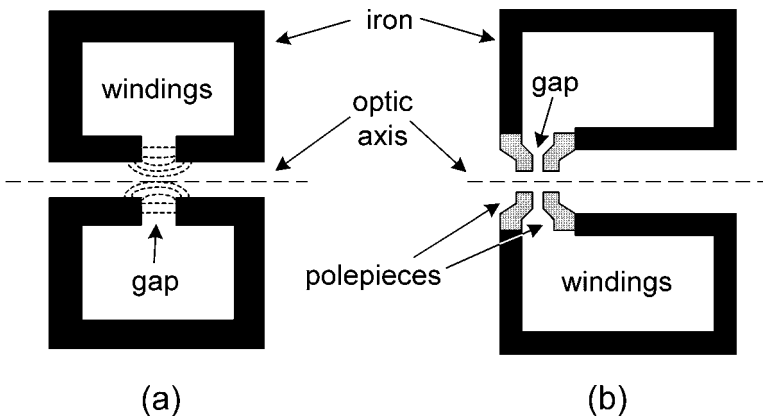


Figure 2-9. (a) Use of ferromagnetic soft iron to concentrate magnetic field within a small volume. (b) Use of ferromagnetic polepieces to further concentrate the field.

A cross section through a typical magnetic lens is shown in Fig. 2-10. Here the optic axis is shown vertical, as is nearly always the case in practice. A typical electron-beam instrument contains several lenses, and stacking them vertically (in a lens **column**) provides a mechanically robust structure in which the weight of each lens acts parallel to the optic axis. There is then no tendency for the column to gradually bend under its own weight, which would lead to lens **misalignment** (departure of the polepieces from a straight-line configuration). The strong magnetic field (up to about 2 Tesla) in each lens gap is generated by a relatively large coil that contains many turns of wire and typically carries a few amps of direct current. To remove heat generated in the coil (due to its resistance), water flows into and out of each lens. Water cooling ensures that the temperature of the lens column reaches a stable value, not far from room temperature, so that thermal expansion (which could lead to column misalignment) is minimized. Temperature changes are also reduced by controlling the temperature of the cooling water within a refrigeration system that circulates water through the lenses in a closed cycle and removes the heat generated.

Rubber **o-rings** (of circular cross section) provide an airtight seal between the interior of the lens column, which is connected to vacuum pumps, and the exterior, which is at atmospheric pressure. The absence of air in the vicinity of the electron beam is essential to prevent collisions and scattering of the electrons by air molecules. Some internal components (such as apertures) must be located close to the optic axis but adjusted in position by external controls. Sliding o-ring seals or thin-metal bellows are used to allow this motion while preserving the internal vacuum.

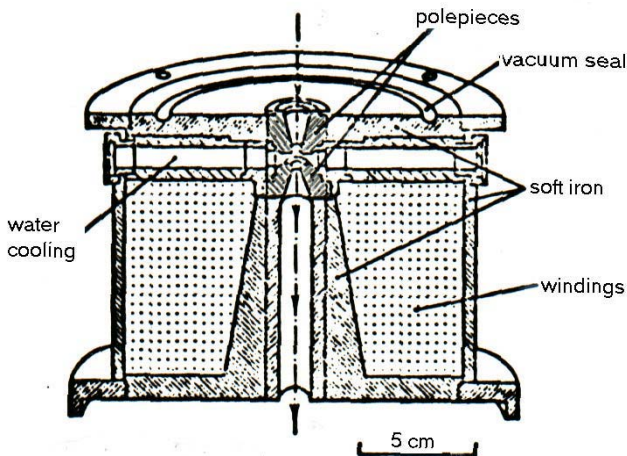


Figure 2-10. Cross section through a magnetic lens whose optic axis (dashed line) is vertical.

2.4 Focusing Properties of a Thin Magnetic Lens

The use of ferromagnetic polepieces results in a focusing field that extends only a few millimeters along the optic axis, so that to a first approximation the lens may be considered thin. Deflection of the electron trajectory can then be considered to take place at a single plane (the principal plane), which allows thin-lens formulas such as Eq. (2.2) and Eq. (2.3) to be used to describe the optical properties of the lens.

The thin-lens approximation also simplifies analysis of the effect of the magnetic forces acting on a charged particle, leading to a simple expression for the **focusing power** (reciprocal of focal length) of a magnetic lens:

$$1/f = [e^2/(8mE_0)] \int B_z^2 dz \quad (2.7)$$

As we are considering electrons, the particle charge e is 1.6×10^{-19} C and mass $m = 9.11 \times 10^{-31}$ kg; E_0 represents the kinetic energy of the particles passing through the lens, expressed in Joule, and given by $E_0 = (e)(V_0)$ where V_0 is the potential difference used to accelerate the electrons from rest. The integral ($\int B_z^2 dz$) can be interpreted as the total area under a graph of B_z^2 plotted against distance z along the optic axis, B_z being the z -component of magnetic field (in Tesla). Because the field is non-uniform, B_z is a function of z and also depends on the lens current and the polepiece geometry.

There are two simple cases in which the integral in Eq. (2.7) can be solved analytically. One of these corresponds to the assumption that B_z has a constant value B_0 in a region $-a < z < a$ but falls abruptly to zero outside this region. The total area is then that of a rectangle and the integral becomes $2aB_0^2$. This rectangular distribution is unphysical but would approximate the field produced by a long solenoid of length $2a$.

For a typical electron lens, a more realistic assumption is that B increases smoothly toward its maximum value B_0 (at the center of the lens) according to a symmetric *bell-shaped* curve described by the **Lorentzian** function:

$$B_z = B_0 / (1 + z^2/a^2) \quad (2.8)$$

As we can see by substituting $z = a$ in Eq. (2.8), a is the half-width at half maximum (HWHM) of a graph of B_z versus z , meaning the distance (away from the central maximum) at which B_z falls to *half* of its maximum value; see Fig. 2-8. Alternatively, $2a$ is the *full* width at half maximum (FWHM) of the field: the length (along the optic axis) over which the field exceeds $B_0/2$. If Eq. (2.8) is valid, the integral in Eq. (2.7) becomes $(\pi/2)aB_0^2$ and the focusing power of the lens is

$$1/f = (\pi/16) [e^2/(mE_0)] aB_0^2 \quad (2.9)$$

As an example, we can take $B_0 = 0.3$ Tesla and $a = 3$ mm. If the electrons entering the lens have been accelerated from rest by applying a voltage $V_0 = 100$ kV, we have $E_0 = eV_0 = 1.6 \times 10^{-14}$ J. Equation (2.9) then gives the focusing power $1/f = 93 \text{ m}^{-1}$ and focal length $f = 11$ mm. Because f turns out to be less than twice the full-width of the field ($2a = 6$ mm) we might question the accuracy of the thin-lens approximation in this case. In fact, more exact calculations (Reimer, 1997) show that the thin-lens formula underestimates f by about 14% for these parameters. For larger B_0 and a , Eqs. (2.7) and (2.9) become unrealistic (see Fig. 2-13 later). In other words, strong lenses must be treated as *thick* lenses, for which (as in light optics) the mathematical description is more complicated.

In addition, our thin-lens formula for $1/f$ is based on non-relativistic mechanics, in which the mass of the electron is assumed to be equal to its rest mass. The relativistic increase in mass (predicted by Einstein's Special Relativity) can be incorporated by replacing E_0 by $E_0 (1 + V_0 / 1022 \text{ kV})$ in Eq. (2.9). This modification increases f by about 1% for each 10 kV of accelerating voltage, that is by 10% for $V_0 = 100$ kV, 20% for $V_0 = 200$ kV, and so on.

Although only approximate, Eq. (2.9) enables us to see how the focusing power of a magnetic lens depends on the strength and spatial extent of the magnetic field and on certain properties of particles being imaged (their kinetic energy, charge and mass). Because the kinetic energy E_0 appears in the denominator of Eq. (2.7), focusing power decreases as the accelerating voltage is increased. As might be expected intuitively, faster electrons are deflected less in the magnetic field.

Because B_0 is proportional to the current supplied to the lens windings, changing this current allows the focusing power of the lens to be varied. This ability to vary the focal length means that an electron image can be focused by adjusting the lens current. However, it also implies that the lens current must be highly stabilized (typically to within a few parts per million) to prevent *unwanted* changes in focusing power, which would cause the image to drift out of focus. In *light optics*, change in f can only be achieved mechanically: by changing the curvature of the lens surfaces (in the case of the eye) or by changing the spacing between elements of a compound lens, as in the zoom lens of a camera.

When discussing qualitatively the action of a magnetic field, we saw that the electrons execute a spiral motion, besides being deflected back toward the optic axis. As a result, the plane containing the exit ray is rotated through an angle ϕ relative to the plane containing the incoming electron. Again making a thin-lens approximation ($a \ll f$) and assuming a Lorentzian field distribution, the equations of motion can be solved to give:

$$\phi = [e/(8mE_0)^{1/2}] \int B_z dz = [e/(8mE_0)^{1/2}] \pi a B_0 \quad (2.10)$$

Using $B_0 = 0.3$ T, $a = 3$ mm, and $V_0 = 100$ kV as before: $\phi = 1.33$ rad = 76° , so the rotation is not unimportant. Note that this rotation is *in addition* to the inversion about the z -axis that occurs when a real image is formed (Fig. 2-5). In other words, the rotation of a *real* electron image, relative to the object, is actually $\pi \pm \phi$ radians.

Note that the image rotation would reverse (*e.g.*, go from clockwise to counterclockwise) if the current through the lens windings were reversed, because B_z (and therefore ϕ) would be reversed in sign. On the other hand, reversing the current does *not* change the focusing power, as the integral in Eq. (2.7) involves B_z^2 , which is always positive. In fact, all of the terms in Eq. (2.7) are positive, implying that we cannot use an axially-symmetric magnetic field to produce the electron-optical equivalent of a diverging (concave) lens, for which the focal length f would have to be negative.

Equations (2.7) – (2.10) apply equally well to the focusing of other charged particles such as protons and ions, provided e and m are replaced by the appropriate charge and mass. Equation (2.7) shows that, for the same lens current and kinetic energy (same potential used to accelerate the particles), the focusing power of a magnetic lens is much less for these particles, whose mass is thousands of times larger than that of the electron. For this reason, **ion optics** commonly involves *electrostatic* lenses.

2.5 Comparison of Magnetic and Electrostatic Lenses

Some of the differences between electrostatic and magnetic lenses (of axial symmetry) are summarized in Table 2-1 and will now be discussed in turn.

Because the electrostatic force on an electron is parallel (or in the case of an electron, antiparallel) to the field and because axially symmetric fields have no tangential component, electrostatic lenses offer the convenience of no image rotation. Their low weight and near-zero power consumption has made them attractive for space-based equipment, such as planetary probes.

The ability of electrostatic lenses to operate with voltages that slowly change (drift) or contain fluctuating components (ripple) is a result of the fact that the voltage supply that is connected to the lens can also be used to accelerate the electrons, as illustrated in Fig. 2-6. If the accelerating voltage V_0 increases, the electrons travel faster; but as it requires a higher lens voltage to focus faster electrons, the two effects cancel (to first order). Electrostatic lenses were therefore preferred in some of the early electron

microscopes, at a time when high-voltage supplies were less stable than is possible today.

On the other hand, the fact that a voltage comparable to the accelerating voltage V_0 must be applied to an electrostatic lens means that insulation and safety problems become severe for $V_0 > 50$ kV. Because higher accelerating voltages permit better image resolution, magnetic lenses are generally preferred for electron microscopy. Magnetic lenses also provide somewhat lower aberrations, for the same focal length, further improving the image resolution. As we will see later in this chapter, lens aberrations are also reduced by making the focal length of the objective lens small, implying a magnetic *immersion* lens with the specimen present *within* the lens field. Such a concept is problematic for an electrostatic objective, where introducing a conducting specimen could greatly modify the electric-field distribution.

Table 2-1. Comparison of electrostatic and electromagnetic lens designs.

Advantages of an electrostatic lens	Advantages of a magnetic lens
No image rotation	Lower lens aberrations
Lightweight, consumes no power	No high-voltage insulation required
Highly stable voltage unnecessary	Can be used as an immersion lens
Easier focusing of ions	

2.6 Defects of Electron Lenses

For a microscope, the most important focusing defects are lens *aberrations*, as they reduce the spatial resolution of the image, even when it has been optimally focused. We will discuss two kinds of **axial aberrations**, those that lead to image blurring even for object points that lie *on the optic axis*. Similar aberrations occur in light optics.

Spherical aberration

The effect of spherical aberration can be defined by means of a diagram that shows electrons arriving at a thin lens after traveling parallel to the optic axis but not necessarily along it; see Fig. 2-11. Those that arrive very *close to* the optic axis (*paraxial* rays, represented by dashed lines in Fig. 2-11) are brought to a focus F, a distance f from the center of the lens, at the **Gaussian**

image plane. When spherical aberration is present, electrons arriving at an appreciable distance x from the axis are focused to a different point F_1 located at a shorter distance f_1 from the center of the lens.

We might expect the axial shift in focus ($\Delta f = f - f_1$) to depend on the initial x -coordinate of the electron and on the degree of imperfection of the lens focusing. Without knowing the details of this imperfection, we can represent the x -dependence in terms of a power series:

$$\Delta f = c_2 x^2 + c_4 x^4 + \text{higher even powers of } x \quad (2.11)$$

with c_2 and c_4 as unknown coefficients. Note that odd powers of x have been omitted: provided the magnetic field that focuses the electrons is axially symmetric, the deflection angle α will be identical for electrons that arrive with coordinates $+x$ and $-x$ (as in Fig. 2-11). This would not be the case if terms involving x or x^3 were present in Eq. (2.11).

From the geometry of the large right-angled triangle in Fig. 2-11,

$$x = f_1 \tan \alpha \approx f \tan \alpha \approx f \alpha \quad (2.12)$$

Here we have assumed that $x \ll f$, taking the angle α to be small, and also that $\Delta f \ll f$, supposing spherical aberration to be a *small* effect for electrons that deviate by no more than a few degrees from the optic axis. These approximations are reasonable for high-voltage electron optics.

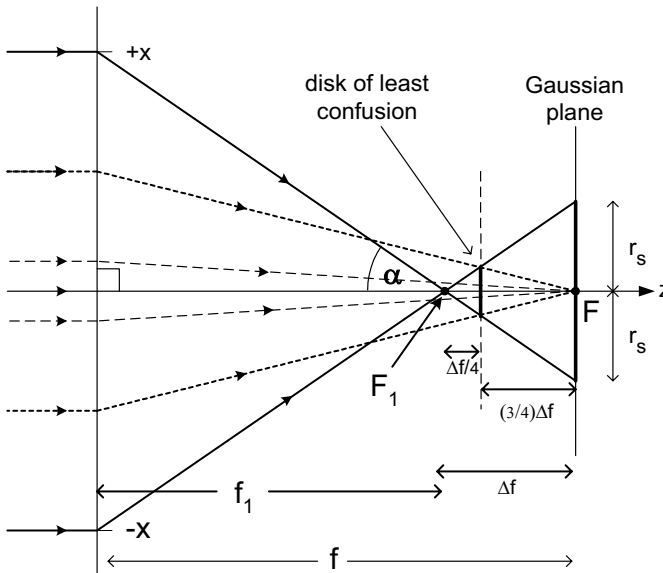


Figure 2-11. Definition of the disk of confusion due to spherical aberration, in terms of the focusing of parallel rays by a thin lens.

When these non-paraxial electrons arrive at the Gaussian image plane, they will be displaced radially from the optic axis by an amount r_s given by:

$$r_s = (\Delta f) \tan \alpha \approx (\Delta f) \alpha \quad (2.13)$$

where we once again assume that α is small. As small α implies small x , we can to a first approximation neglect powers higher than x^2 in Eq. (2.11) and combine this equation with Eqs. (2.12) and (2.13) to give:

$$r_s \approx [c_2 (f\alpha)^2] \alpha = c_2 f^2 \alpha^3 = C_s \alpha^3 \quad (2.14)$$

in which we have combined c_2 and f into a single constant C_s , known as the **coefficient of spherical aberration** of the lens. Because α (in radian) is dimensionless, C_s has the dimensions of length.

Figure 2-11 illustrates a limited number of off-axis electron trajectories. More typically, we have a broad entrance beam of circular cross-section, with electrons arriving at the lens with all radial displacements (*between* zero and some value x) within the x - z plane (that of the diagram), within the y - z plane (perpendicular to the diagram), and within all intermediate planes that contain the optic axis. Due to the axial symmetry, all these electrons arrive at the Gaussian image plane *within* the disk of confusion (radius r_s). The angle α now represents the *maximum* angle of the focused electrons, which might be determined by the internal diameter of the lens bore or by a circular aperture placed in the optical system.

Figure 2-11 is directly relevant to a scanning electron microscope (SEM), where the objective lens focuses a near-parallel beam into an electron probe of very small diameter at the specimen. Because the spatial resolution of the secondary-electron image cannot be better than the probe diameter, spherical aberration might be expected to limit the spatial resolution to a value of the order of $2r_s$. In fact, this conclusion is too pessimistic. If the specimen is advanced toward the lens, the illuminated disk gets smaller and at a certain location (represented by the dashed vertical line in Fig. 2-11), its diameter has a minimum value ($= r_s/2$) corresponding to the **disk of least confusion**. Advancing the specimen any closer to the lens would make the disk larger, due to contributions from medium-angle rays, shown dotted in Fig. 2-11.

In the case of a transmission electron microscope (TEM), a relatively broad beam of electrons arrives at the specimen, and an objective lens simultaneously images each object point. Figure 2.11 can be made more applicable by first imagining the lens to be weakened slightly, so that F is the Gaussian image of an object point G located at a large but finite distance u from the lens, as in Fig. 2-12a. Even so, the diagram represents the case of large *demagnification* ($u/f \approx M \ll 1$), not $M \gg 1$ as required for a microscope. To describe the TEM situation, we can reverse the ray paths, a

procedure that is permissible in both light and electron optics, resulting in Fig. 2-12b. By adding extra dashed rays as shown, Fig. 2-12b illustrates how electrons emitted from two points a distance $2r_s$ apart are focused into two magnified disks of confusion in the image (shown on the left) of radius Mr_s and separation $2Mr_s$. Although these disks touch at their periphery, the image would still be recognizable as representing two separate point-like objects in the specimen. If the separation between the object points is now reduced to r_s , the disks overlap substantially, as in Fig. 2-12c. For a further reduction in spacing, the two separate point objects would no longer be distinguishable from the image, and so we take r_s as the spherical-aberration limit to the **point resolution** of a TEM objective lens. This approximates to the Rayleigh criterion (Section 1.1); the current-density distribution in the image consists of two overlapping peaks with about 15% dip between them.

Spherical aberration occurs in TEM lenses *after* the objective but is much less important. This situation arises from the fact that each lens *reduces* the maximum angle of electrons (relative to the optic axis) by a factor equal to its magnification (as illustrated in Fig 2.12b), while the spherical-aberration blurring depends on the *third power* of this angle, according to Eq. (2.14).

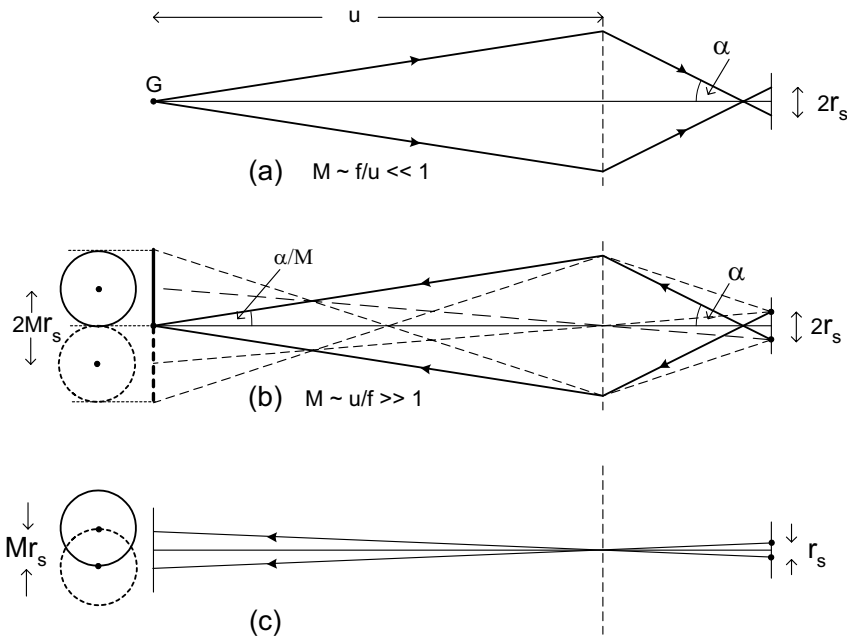


Figure 2-12. (a) Ray diagram similar to Fig. 2-11, with the object distance u large but finite. (b) Equivalent diagram with the rays reversed, showing two image disks of confusion arising from object points whose separation is $2r_s$. (c) Same diagram but with object-point separation reduced to r_s so that the two points are barely resolved in the image (Rayleigh criterion).

So far, we have said nothing about the *value* of the spherical-aberration coefficient C_s . On the assumption of a Lorentzian (bell-shaped) field, C_s can be calculated from a somewhat-complicated formula (Glaeser, 1952). Figure 2.13 shows the calculated C_s and focal length f as a function of the maximum field B_0 , for 200kV accelerating voltage and a field half-width of $a = 1.8$ mm. The thin-lens formula, Eq. (2.9), is seen to be quite good at predicting the focal length of a weak lens (low B_0) but becomes inaccurate for a strong lens. For the weak lens, $C_s \approx f \approx$ several mm; but for a strong lens ($B_0 = 2$ to 3 T, as used for a TEM objective), C_s falls to about $f/4$. If we take $f = 2$ mm, so that $C_s \approx 0.5$ mm, and require a point resolution $r_s = 1$ nm, the maximum angle of the electrons (relative to the optic axis) must satisfy: $C_s \alpha^3 \approx r_s$, giving $\alpha \approx 10^{-2}$ rad = 10 mrad. This low value justifies our use of small-angle approximations in the preceding analysis.

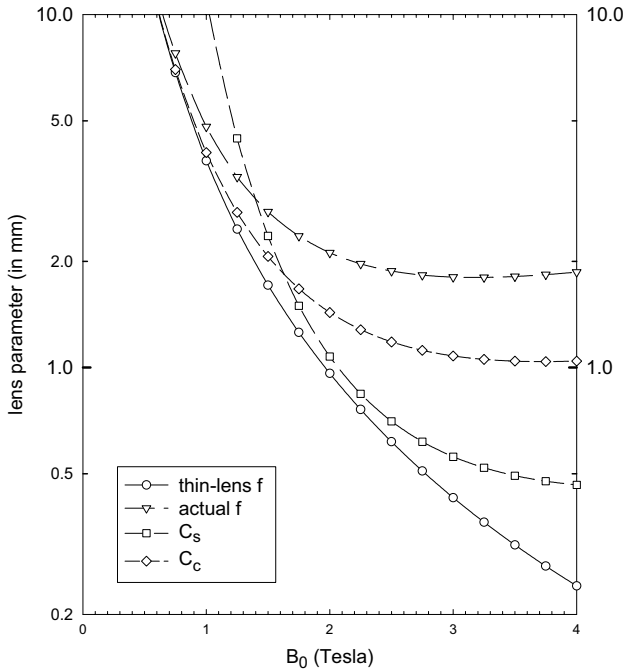


Figure 2-13. Focal length and coefficients of spherical and chromatic aberration for a magnetic lens containing a Lorentzian field with peak field B_0 and half-width $a = 1.8$ mm, focusing 200keV electrons. Values were calculated from Eq. (2.7) and from Glaeser (1952).

The basic physical properties of a magnetic field dictate that the spherical aberration of an axially-symmetric electron lens cannot be eliminated through careful design of the lens polepieces. However, spherical aberration can be *minimized* by using a strong lens (small f). The smallest possible focal length is determined by the maximum field ($B_0 \approx 2.6$ Tesla) obtainable, limited by magnetic saturation of the lens polepieces. The radius r_s of the disk of confusion is also reduced by using an aperture in the lens column to limit the maximum angular deviation α of electrons from the optic axis.

Chromatic aberration

In light optics, chromatic aberration occurs when there is a spread in the wavelength of the light passing through a lens, coupled with a variation of refractive index with wavelength (dispersion). In the case of an electron, the de Broglie wavelength depends on the particle momentum, and therefore on its kinetic energy E_0 , while Eq. (2.7) shows that the focusing power of a magnetic lens depends inversely on the kinetic energy. So if electrons are present with different kinetic energies, they will be focused at a different distances from a lens; for any image plane, there will be a *chromatic* disk of confusion rather than a point focus. The spread in kinetic energy can arise from several causes.

(1) Different kinetic energies of the electrons emitted from the source. For example, electrons emitted by a heated-filament source have a **thermal spread** ($\approx kT$, where T is the temperature of the emitting surface) due to the statistics of the electron-emission process.

(2) Fluctuations in the potential V_0 applied to accelerate the electrons. Although high-voltage supplies are stabilized as well as possible, there is still some **drift** (slow variation) and **ripple** (alternating component) in the accelerating voltage, and therefore in the kinetic energy eV_0 .

(3) Energy loss due to **inelastic scattering** in the specimen, a process in which energy is transferred from an electron to the specimen. This scattering is also a statistical process: not all electrons lose the same amount of energy, resulting in an energy spread within the transmitted beam. Because the TEM *imaging* lenses focus electrons *after* they have passed through the specimen, inelastic scattering will cause chromatic aberration in the magnified image.

We can estimate the radius of the *chromatic* disk of confusion by the use of Eq. (2.7) and thin-lens geometric optics, ignoring spherical aberration and other lens defects. Consider an axial point source P of electrons (distance u from the lens) that is focused to a point Q in the image plane (distance v

from the lens) for electrons of energy E_0 as shown in Fig. 2-14. Because $1/f$ increases as the electron energy decreases, electrons of energy $E_0 - \Delta E_0$ will have an image distance $v - \Delta v$ and arrive at the image plane a radial distance r_i from the optic axis. If the angle β of the arriving electrons is small,

$$r_i = \Delta v \tan \beta \approx \beta \Delta v \quad (2.15)$$

As in the case of spherical aberration, we need to know the x -displacement of a second point object P' whose disk of confusion partially overlaps the first, as shown in Fig. 2-14. As previously, we will take the required displacement in the image plane to be *equal* to the disk radius r_i , which will correspond to a displacement *in the object plane* equal to $r_c = r_i/M$, where M is the image magnification given by:

$$M = v/u = \tan \alpha / \tan \beta \approx \alpha / \beta \quad (2.16)$$

From Eqs. (2.15) and (2.16), we have:

$$r_c \approx \beta \Delta v / M \approx \alpha \Delta v / M^2 \quad (2.17)$$

Assuming a thin lens, $1/u + 1/v = 1/f$ and taking derivatives of this equation (for a fixed object distance u) gives: $0 + (-2) v^{-2} \Delta v = (-2) f^{-2} \Delta f$, leading to:

$$\Delta v = (v^2/f^2) \Delta f \quad (2.18)$$

For $M \gg 1$, the thin-lens equation, $1/u + 1/(Mu) = 1/f$, implies that $u \approx f$ and $v \approx Mf$, so Eq. (2.18) becomes $\Delta v \approx M^2 \Delta f$ and Eq. (4.7) gives:

$$r_c \approx \alpha \Delta f \quad (2.19)$$

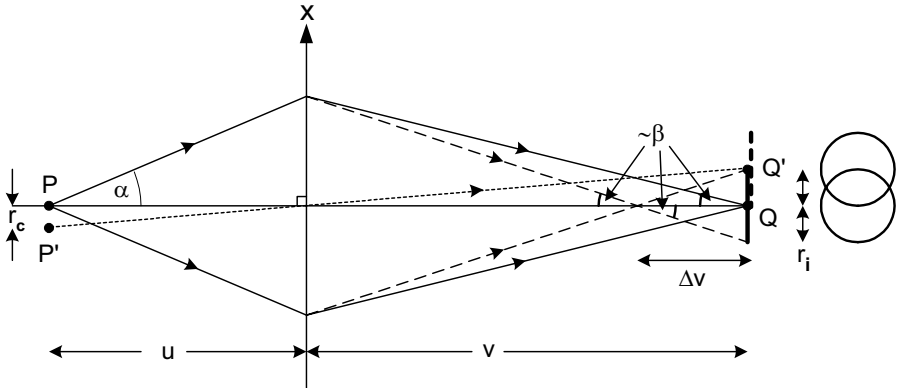


Figure 2-14. Ray diagram illustrating the change in focus and the disk of confusion resulting from chromatic aberration. With two object points, the image disks overlap; the Rayleigh criterion (about 15% reduction in intensity between the current-density maxima) is satisfied when the separation PP' in the object plane is given by Eq. (2.20).

From Eq. (2.7), the focal length of the lens can be written as $f = A E_0$ where A is independent of electron energy, and taking derivatives gives: $\Delta f = A \Delta E_0 = (f/E_0) \Delta E_0$. The loss of spatial resolution due to chromatic aberration is therefore:

$$r_c \approx \alpha f (\Delta E_0 / E_0) \quad (2.20)$$

More generally, a **coefficient of chromatic aberration** C_c is defined by the equation:

$$r_c \approx \alpha C_c (\Delta E_0 / E_0) \quad (2.21)$$

Our analysis has shown that $C_c = f$ in the thin-lens approximation. A more exact (thick-lens) treatment gives C_c slightly smaller than f for a weak lens and typically $f/2$ for a strong lens; see Fig. 2-13. As in the case of spherical aberration, chromatic aberration cannot be eliminated through lens design but is minimized by making the lens as strong as possible (large focusing power, small f) and by using an angle-limiting aperture (restricting α). High electron-accelerating voltage (large E_0) also reduces the chromatic effect.

Axial astigmatism

So far we have assumed complete axial symmetry of the magnetic field that focuses the electrons. In practice, lens polepieces cannot be machined with perfect accuracy, and the polepiece material may be slightly inhomogeneous, resulting in local variations in relative permeability. In either case, the departure from cylindrical symmetry will cause the magnetic field at a given radius r from the z -axis to depend on the *plane of incidence* of an incoming electron (*i.e.*, on its **azimuthal** angle ϕ , viewed along the z -axis). According to Eq. (2.9), this difference in magnetic field will give rise to a difference in focusing power, and the lens is said to suffer from **axial astigmatism**.

Figure 2.15a shows electrons leaving an *on-axis* object point P at equal angles to the z -axis but traveling in the x - z and y - z planes. They cross the optic axis at different points, F_x and F_y , displaced along the z -axis. In the case of Fig. 2-15a, the x -axis corresponds to the *lowest* focusing power and the perpendicular y -direction corresponds to the *highest* focusing power.

In practice, electrons leave P with *all* azimuthal angles and at all angles (up to α) relative to the z -axis. At the plane containing F_y , the electrons lie within a **caustic figure** that approximates to an ellipse whose long axis lies parallel to the x -direction. At F_x they lie within an ellipse whose long axis points in the y -direction. At some intermediate plane F, the electrons define a circular disk of confusion of radius R , rather than a single point. If that plane is used as the image (magnification M), astigmatism will limit the point resolution to a value R/M .

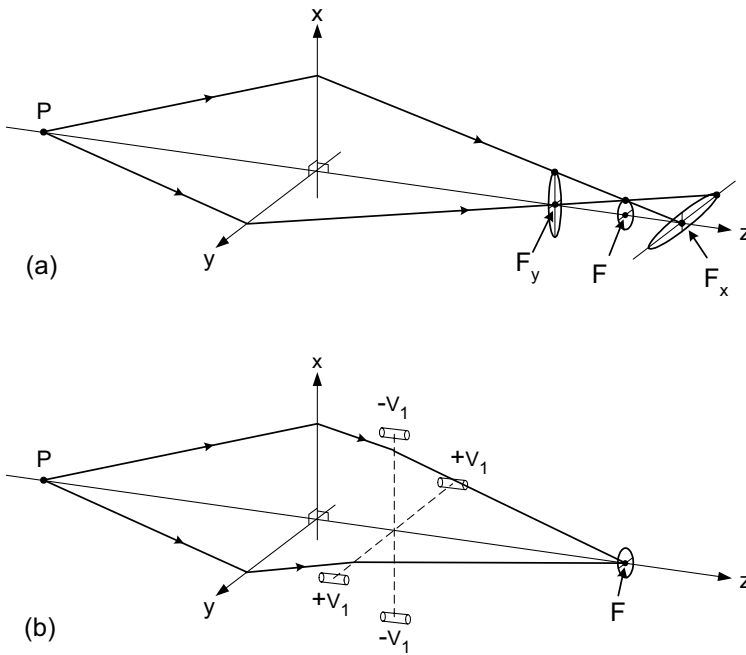


Figure 2-15. (a) Rays leaving an axial image point, focused by a lens (with axial astigmatism) into ellipses centered around F_x and F_y or into a circle of radius R at some intermediate plane. (b) Use of an electrostatic stigmator to correct for the axial astigmatism of an electron lens.

Axial astigmatism also occurs in the human eye, when there is a lack of axial symmetry. It can be *corrected* by wearing lenses whose focal length differs with azimuthal direction by an amount just sufficient to compensate for the azimuthal variation in focusing power of the eyeball. In *electron* optics, the device that corrects for astigmatism is called a **stigmator** and it takes the form of a weak **quadrupole lens**.

An *electrostatic* quadrupole consists of four electrodes, in the form of short conducting rods aligned parallel to the z -axis and located at equal distances along the $+x$, $-x$, $+y$, and $-y$ directions; see Fig. 2-15b. A power supply generating a voltage $-V_1$ is connected to the two rods that lie in the x - z plane and electrons traveling in that plane are repelled *toward* the axis, resulting in a *positive* focusing power (convex-lens effect). A potential $+V_1$ is applied to the other pair, which therefore *attract* electrons traveling in the y - z plane and provide a *negative* focusing power in that plane. By combining the stigmator with an astigmatic lens and choosing V_1 appropriately, the focal length of the system in the x - z and y - z planes can be made equal; the two foci F_x and F_y are brought together to a single point and the axial astigmatism is eliminated, as in Fig. 2-15b.

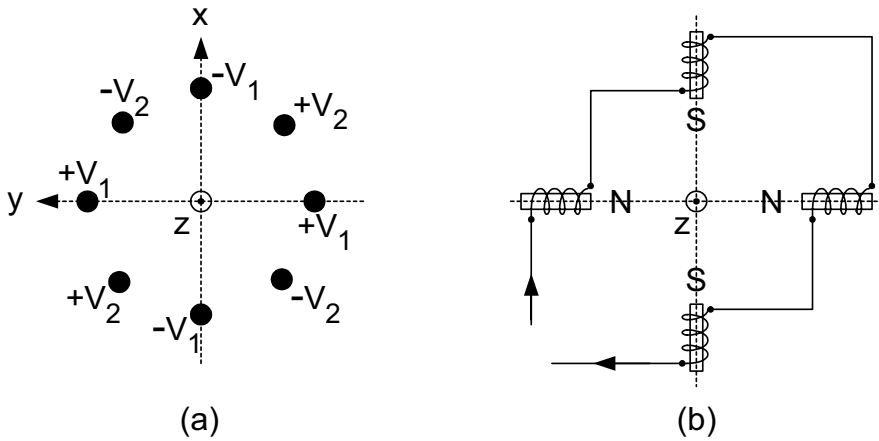


Figure 2-16. (a) Electrostatic stigmator, viewed along the optic axis; (b) magnetic quadrupole, the basis of an electromagnetic stigmator.

In practice, we cannot predict which azimuthal direction corresponds to the smallest or the largest focusing power of an astigmatic lens. Therefore the *direction* of the stigmator correction must be adjustable, as well as its strength. One way of achieving this is to mechanically rotate the quadrupole around the z -axis. A more convenient arrangement is to add four more electrodes, connected to a second power supply that generates potentials of $+V_2$ and $-V_2$, as in Fig. 2-16a. Varying the magnitude and polarity of the two voltage supplies is equivalent to varying the strength and orientation of a single quadrupole while avoiding the need for a rotating vacuum seal.

A more common form of stigmator consists of a *magnetic* quadrupole: four short solenoid coils with their axes pointing toward the optic axis. The coils that generate the magnetic field are connected in series and carry a common current I_1 . They are wired so that north and south magnetic poles face each other, as in Fig. 2-16b. Because the magnetic force on an electron is perpendicular to the magnetic field, the coils that lie along the x -axis deflect electrons in the y -direction and *vice versa*. In other respects, the magnetic stigmator acts similar to the electrostatic one. Astigmatism correction could be achieved by adjusting the current I_1 and the azimuthal orientation of the quadrupole, but in practice a second set of four coils is inserted at 45° to the first and carries a current I_2 that can be varied independently. Independent adjustment of I_1 and I_2 enables the astigmatism to be corrected without any mechanical rotation.

The stigmators found in electron-beam columns are *weak* quadrupoles, designed to correct for *small* deviations of in focusing power of a much stronger lens. Strong quadrupoles are used in synchrotrons and nuclear-particle accelerators to focus high-energy electrons or other charged particles. Their focusing power is positive in one plane and negative (diverging, equivalent to a concave lens) in the perpendicular plane. However, a series combination of *two* quadrupole lenses can result in an overall convergence in both planes, without image rotation and with less power dissipation than required by an axially-symmetric lens. This last consideration is important in the case of particles heavier than the electron.

In light optics, the surfaces of a glass lens can be machined with sufficient accuracy that *axial* astigmatism is negligible. But for rays coming from an *off-axis* object point, the lens appears elliptical rather than round, so *off-axis* astigmatism is unavoidable. In electron optics, this kind of astigmatism is not significant because the electrons are confined to small angles relative to the optic axis (to avoid excessive spherical and chromatic aberration). Another off-axis aberration, called *coma*, is of some importance in a TEM if the instrument is to achieve its highest possible resolution.

Distortion and curvature of field

In an undistorted image, the distance R of an image point from the optic axis is given by $R = M r$, where r is the distance of the corresponding object point from the axis, and the image magnification M is a constant. Distortion changes this ideal relation to:

$$R = M r + C_d r^3 \quad (2.22)$$

where C_d is a constant. If $C_d > 0$, each image point is displaced outwards, particularly those further from the optic axis, and the entire image suffers from pincushion distortion (Fig. 2-2c). If $C_d < 0$, each image point is displaced inward relative to the ideal image and barrel distortion is present (Fig. 2-2b).

As might be expected from the third-power dependence in Eq. (2.22), distortion is related to spherical aberration. In fact, an axially-symmetric electron lens (for which $C_s > 0$) will give $C_d > 0$ and pincushion distortion. Barrel distortion is produced in a two-lens system in which the second lens magnifies a *virtual* image produced by the first lens. In a multi-lens system, it is therefore possible to combine the two types of distortion to achieve a distortion-free image.

In the case of magnetic lenses, a third type of distortion arises from the fact that the image rotation ϕ may depend on the distance r of the object

point from the optic axis. This spiral distortion was illustrated in Fig. 2-2c. Again, compensation is possible in a multi-lens system.

For most purposes, distortion is a less serious lens defect than aberration, because it does not result in a loss of image detail. In fact, it may not be noticeable unless the microscope specimen contains straight-line features. In some TEMs, distortion is observed when the final (projector) lens is operated at reduced current (therefore large C_s) to achieve a low overall magnification.

Curvature of field is not a serious problem in the TEM or SEM, because the angular deviation of electrons from the optic axis is small. This results in a large *depth of focus* (the image remains acceptably sharp as the plane of viewing is moved along the optic axis) as we will discuss in Chapter 3.

<http://www.springer.com/978-0-387-25800-3>

Physical Principles of Electron Microscopy

An Introduction to TEM, SEM, and AEM

Egerton, R.F.

2005, XII, 202 p. 122 illus., Hardcover

ISBN: 978-0-387-25800-3